

## Effect of Annealing Heat Treatment to Characteristics of ALDC8 (Al-Si-Cu) Alloy

Kyung Man Moon<sup>1</sup>, Sung-Yul Lee<sup>1</sup>, Myeong Hoon Lee<sup>2</sup>, Tae-Sil Baek<sup>3</sup>, and Jae-Hyun Jeong<sup>4,†</sup>

<sup>1</sup>Dept. of Marine Equipment Engineering, Korea Maritime and Ocean University Dongsam-2dong Youngdo-ku Busan 606-791, Korea

<sup>2</sup>Dept. of Marine System Engineering, Korea Maritime and Ocean University

<sup>3</sup>Dept. of Steel Industry, Pohang College, 60 Sindukro Hughaeup Bukgu, Pohang City, Gyeong Buk, Korea

<sup>4</sup>Dept. of Mechanical & Energy Systems Engineering, Korea Maritime University, Dong Sam-Dong, Yong Do-ku, Busan, Korea

(Received January 20, 2015; Revised November 09, 2015; Accepted November 10, 2015)

ALDC8 (Al-Si-Cu) alloy has been often corroded with pattern of intergranular corrosion in corrosive environments. Thus, in order to improve its corrosion resistance, the effect of annealing heat treatment to corrosion resistance and hardness was investigated with parameters of heating temperatures such as 100 °C, 200 °C, 300 °C, 400 °C and 500 °C for 1hr. The hardness was varied with annealing temperature and slightly decreased with annealing heat treatment. However, the relation between annealing temperature and hardness agreed not well each other. Corrosion potential was shifted to noble direction and corrosion current density was also decreased with increasing annealing temperature. Moreover, both AC impedance at 10 mHz and polarization resistance on the cyclic voltammogram curve were also increased with increasing annealing temperature. Furthermore, intergranular corrosion was somewhat observed in non heat treatment as well as annealing temperatures at 100 °C, 200 °C and 300 °C, while, intergranular corrosion was not nearly observed at annealing temperature of 400 °C, 500 °C. Consequently, it is considered that the annealing heat treatment of ALDC8 alloy may be an available method not only to inhibit its intergranular corrosion but also to improve its corrosion resistance.

**Keywords :** *intergranular corrosion, annealing heat treatment, cyclic voltammogram, AC impedance, corrosion current density*

### 1. Introduction

Al has been widely used as an industrial material for long years<sup>1)</sup>. Moreover, Al not only is easily casted, but also has the good corrosion resistance in both acidic and neutral solution. However the mechanical property of the high pure Al was slightly poor because its crystal structure is a face centered cubic lattice<sup>2)</sup>. Therefore, the mechanical properties such as strength, hardness have been considerably improved by Al alloy added with small amount of component such as Mn, Mg, Si and Cr etc. However, when Al alloys are being used in severe corrosive environment, several types of corrosion such as pitting, intergranular, stress and galvanic corrosions etc. were sometimes appeared inevitably. Hence, the studies on both the kinds of alloying elements and controlling of their amount as well as an optimum heat treatment method have been continuously examined<sup>3-12)</sup>. In spite of these studies, it is well known that ALDC8 (Al-Si-Cu) alloy is often cor-

roded as a form of intergranular corrosion in marine environment compared to other alloy such as ALDC3 (Al-Si), ALDC5 (Al-Mg) alloys. This is because Cu as an alloying element is larger than other alloy, that is, compared to ALDC3 (Al-Si), ALDC5 (Al-Mg) alloys

Therefore, we investigated the effect of annealing heat treatment on corrosion resistance and hardness of ALDC8 (Al-Si-Cu) alloy. Consequently, it is considered that the results of this study may serve as a good available reference data set for successful information on the mechanical and corrosion characteristics when the annealing heat treatment is performed on the ALDC8 (Al-Si-Cu) alloy

### 2. Experimental Procedure

**Table 1. Chemical composition of ALDC8 (Al-Si-Cu) alloy (wt %)**

Cu	Si	Mg	Zn	Fe	Mn	Ni	Sn	Al
2.5	11.5	0.3	1.0	0.9	0.5	0.5	0.3	Residual

<sup>†</sup> Corresponding author: jhjeong@kmou.ac.kr

The main chemical components of ALDC8 (Al-Si-Cu) alloy are Si 11.5 %, Cu 2.5 % as shown in Table 1. Hence, this is thought to be heat treatable to improve its mechanical property and corrosion resistance. The annealing treatment was carried out with various temperatures such as 100 °C, 200 °C, 300 °C, 400 °C and 500 °C for 1 hr. The size of test specimen for electrochemical and mechanical measurements was manufactured with size of 2 cm × 2 cm, and then, 1 cm<sup>2</sup> for working surface is exposed in center area of the specimen, and the other surface was insulated with epoxy coating.

Corrosion potential and polarization curves (scan speed: 1 mV/s), cyclic voltammogram (scan speed: 30 mV/s) and AC impedance were measured through CMS-100 system (Gamry Instruments, Inc. U.K). Test solution was the natural sea water and its temperature was nearly maintained at 25±2 °C.

The microstructure of the surface after annealing heat treatment and corroded surface after drawing of anodic polarization curve were observed by SEM image (Model: SV35, Sometch, Com, Ltd). The surface hardness was also measured depending annealing heat treatment. Vickers hardness was measured three times in center area of the test specimen, and obtained their average values at each annealing temperature.

### 3. Results and Discussion

Fig. 1 shows the morphologies of the surface microstructure after annealing heat treatment with various temperatures. The microstructure of the non-heat treated specimen consisted of a dendrite of  $\alpha$  phase with white color and eutectic structure mixed with Si and CuAl<sub>2</sub> with black color<sup>13)</sup> However  $\alpha$  phase increased slightly with increasing of annealing temperature, in particular, in the annealing temperature at 500 °C,  $\alpha$  phase was considerably increased than that of other annealing temperature, while,

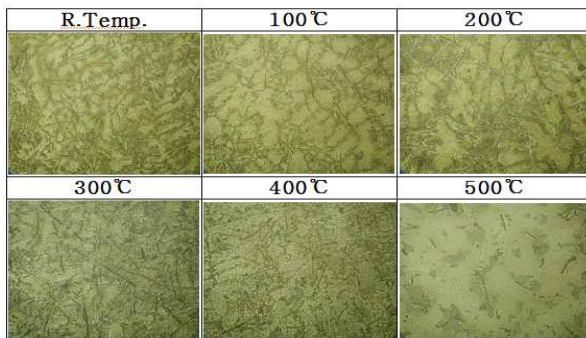


Fig. 1. Morphologies of microstructures with various annealing temperatures.

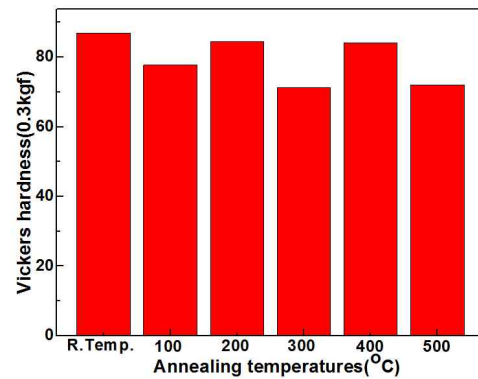


Fig. 2. Variation of hardness with various annealing temperatures.

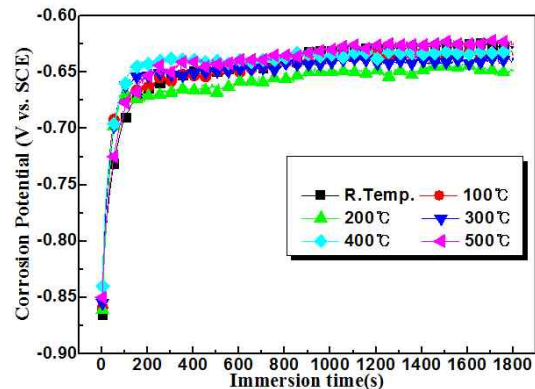


Fig. 3. Variation of corrosion potentials with immersion time in sea water solution.

the eutectic structure of Si and CuAl<sub>2</sub> with black color was significantly decreased compared to those of non-heat treated or heat treated specimens in the other annealing temperatures. It is considered that this result may be caused in a little effect leading inhibition of creation of secondary phases (eutectic structure of Si and CuAl<sub>2</sub>) by annealing heat treatment.

Fig. 2 shows variation of hardness with various annealing temperatures. The hardness was slightly decreased with increasing annealing temperature with heat treatment compared to non-heat treatment. However, the relationship between annealing temperature and hardness matched not well each other, for instance, the hardness at both 200 °C and 400 °C temperatures exhibited more or less higher values rather than those of 100 °C and 300 °C.

Fig. 3 shows variation of corrosion potentials with immersion time in seawater solution.

The corrosion potential was immediately shifted to noble direction as soon as immersion, and then, sustained nearly the stable values against all test specimens. This result is considered to be demonstrated that moving of the noble potential was resulted in oxide film creation. Moreover, it is reported that Al alloy have a good corro-

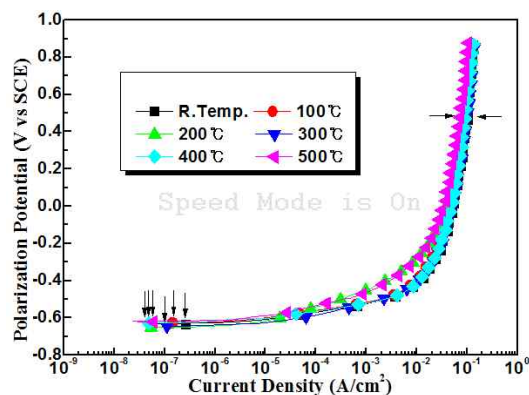


Fig. 4. Comparison of anodic polarization curves with various annealing temperatures in natural seawater solution.

sion resistance in neutral solution compared to acidic or alkali aqueous solution<sup>14</sup>). Furthermore, the corrosion potential in annealing heat treatment at 500 °C exhibited the noblest value of corrosion potential. As a result, it is assumed that the annealing heat treatment at 500 °C indicated qualitatively the best corrosion resistance compared to the other annealing temperatures. By the way, we have discussed about microstructures in previous Fig. 1, that is,  $\alpha$  phase with white color in the annealing temperature at 500 °C was considerably increased than those of other annealing temperatures, while, the eutectic structure of Si and CuAl<sub>2</sub> with black color was significantly decreased than those of both the non-heat treatment and the other annealing temperatures. Therefore, it seems that  $\alpha$  phase with white color and eutectic structure of Si and CuAl<sub>2</sub> with black color may increase and decrease the corrosion resistance, respectively.

Fig. 4 shows variation of anodic polarization curves with various annealing temperatures in natural seawater solution. As shown in Fig. 4, all polarization curves showed nearly same patterns irrespective of annealing temperatures or non-heat treatment. In addition, the anodic polarization curve rapidly shifted to upper direction nearly same as that of passivity pattern from applied current density at about  $4 \times 10^{-2}$  A/cm<sup>2</sup>. This is considered to be formation of resistance polarization caused by deposition of corrosive products or concentration polarization on the surface during drawing of anodic polarization curve. As shown in Fig. 4, in the case of annealing temperature at 500 °C, the current density indicating as horizontal arrows exhibited more or less the smallest value than the other annealing temperatures.

In this study, the surface of the test specimen of ALDC 8 alloy may be deposited with oxide film like Al<sub>2</sub>O<sub>3</sub> in seawater solution, thereby anodic polarization curve is

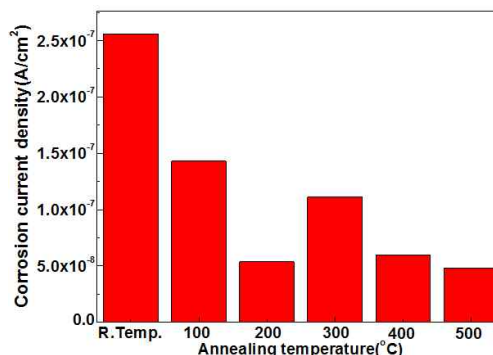


Fig. 5. Comparison of corrosion current densities with various annealing temperatures.

able to involve large amount of resistance polarization due to the oxide film. As a result, the corrosion property by using Tafel extrapolation method could not be correctly calculated in all specimens, that is, non heat treated or heat treated specimens. Moreover, the vertical arrows shown in Fig. 4 indicate the current densities corresponding to corrosion potentials. This is because anodic polarization curve was drawn from corrosion potential at the beginning. Therefore, it is suggested that the current densities corresponding to corrosion potentials can be assumed as the approximate values of corrosion current densities<sup>15</sup>).

Fig. 5 shows approximate values of corrosion current densities obtained from the vertical arrows of Fig. 4. The approximate values of corrosion current densities obtained by annealing heat treatment represented relatively smaller values than that of nonheat treatment. In particular, in the case of annealing temperature at 500 °C, the approximate value of the corrosion current density exhibited the smallest value, and the value of annealing temperature at 200 °C followed the value of annealing temperature at 500 °C

Fig. 6 shows variation of 1st cyclic voltammogram with various annealing temperatures. As shown in Fig. 6, all cyclic polarization curves in the case of annealing treatment were located at the left side compared to non-heat treatment. This means that the polarization resistance of the cyclic voltammogram curve in the case of annealing heat treatment is larger than that of the non heat treatment. Fig. 7 shows variation of 15<sup>th</sup> cyclic voltammogram with various annealing temperatures. The pattern of 15<sup>th</sup> cyclic voltammogram curve was also nearly same as that of Fig. 6. As a result, the corrosion resistance is considered to be increased with increasing the polarization resistance.

Fig. 8 shows variation of AC impedance with various annealing temperatures. In all annealing temperatures ex-

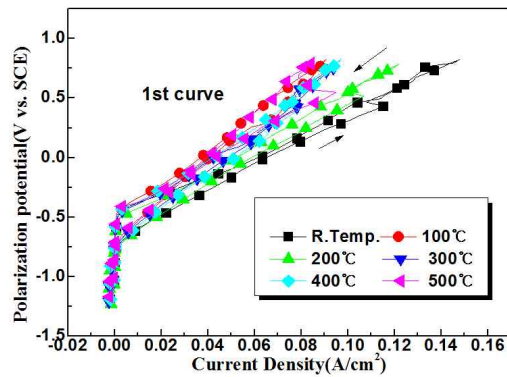


Fig. 6. Variation of 1<sup>st</sup> cyclic voltammogram curves with various annealing temperatures.

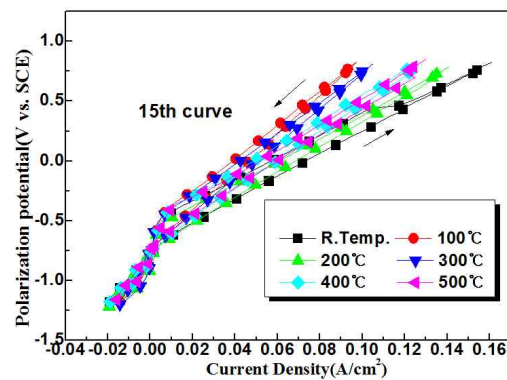


Fig. 7. Variation of 15<sup>th</sup> cyclic voltammogram curves with various annealing temperatures.

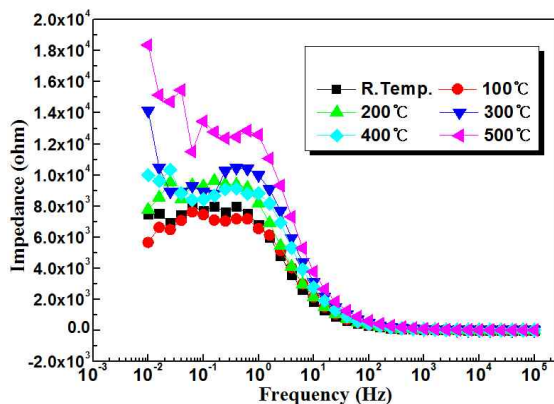


Fig. 8. Variation of bode plots with various annealing temperatures.

cept only 100 °C, the value of AC impedance at 10 mHz was larger than that of non heat treatment, and AC impedance in annealing temperature at 500 °C also indicated the highest value among the annealing temperatures. These results suggest that the corrosion resistance is also increased with increasing AC impedance through annealing treatment.

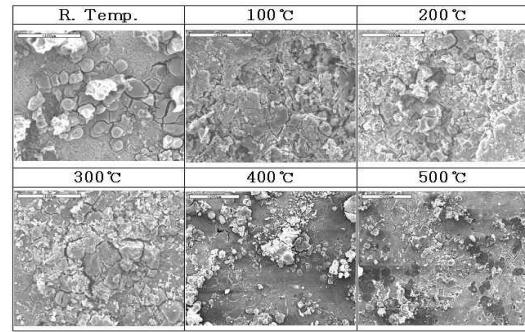


Fig. 9. SEM photographs of corroded surface after drawing anodic polarization curves with various annealing temperatures(x500).

Fig. 9 shows SEM morphologies of the corroded surface after measurement of anodic polarization curves. As shown in these images, the intergranular corrosion was observed at annealing temperatures of 100 °C, 200 °C, 300 °C, and non-heat treatment. However, intergranular corrosion was not nearly observed at annealing temperatures of 400 °C and, 500 °C. It is well known that the intergranular corrosion generally occurred at grain boundary because inclusion like  $\text{CuAl}_2$  located at grain boundary is selectively corroded as an anode. Therefore, annealing at 400 °C and 500 °C inhibits the formation of  $\text{CuAl}_2$ , improving the intergranular corrosion<sup>3,16</sup>.

#### 4. Conclusions

The hardness of the surface was slightly decreased with annealing heat treatment compared to non heat treatment. However, the corrosion resistance was considerably improved in all over the annealing temperatures. Furthermore, the intergranular corrosion was also inhibited in the annealing temperatures at both 400 °C and, 500 °C. Consequently, it is suggested that inhibition of  $\text{CuAl}_2$  by annealing improved corrosion resistance

#### References

1. H. Y. Lee, Metal Corrosion Engineering, p. 262, Yun kyung Munhwa Publication Co. Ltd., Seoul (1999).
2. S. K. Suriyama, Non-metal material Engineering, p. 142, Korona. Publication Co. Ltd., Japan (1975).
3. Mars. G. Fontana, Corrosion Engineering, p. 516, McGraw-Hill Book company, New York (1986).
4. Deny A. Jones, Principles and Prevention of Corrosion, p. 618, Pearson Education, United States (1996).
5. J. W. Martin, Precipitation Hardening, p. 353, Pergamon Press Oxford, New York (1968).
6. Y. Murakami, Fundamentals and Industrial Technologies of Aluminum Materials, p. 252, Light Metals Association, Japan (1985).

7. Y. Murakami, *proceedings of the Advanced Materials and Technology 2<sup>nd</sup> International Conference*, p. 113, Kobe, Japan (1991).
8. A. Hellawell, supplementary Volume 2 of the Encyclopedia of Material Science and Engineering, p. 115, Oxford Pergamon (1990).
9. W. L Phillips, *Annotated Equilibrium Diagram of Some Aluminum Alloy Systems, Monograph*, London Int. Metals. **35**, 57 (1959).
10. A. Sakamoto, *proceedings of the Advanced Materials and Technology 2<sup>nd</sup> International Conference*, p. 165, New Composites, Hyogo, Japan (1991).
11. E. A. Starke, *proceedings of the Materials Science*, p. 208, ASM, Metals Park, Ohio (1979).
12. J. Gilbert, K. Elwin and L. Rooy, *ASM international Materials*, p. 61, OH 44073-002 (1965).
13. S. K. Suriyama, *Non metal material Engineering*, p. 152, Korona Publication Co. Ltd., Japan (1975).
14. N. J. Beak, *Metal Material Engineering*, p. 260, Kawang Rim Publication Co. Ltd., Seoul (1983).
15. K. M. Moon, J. P. Won, D. H. Park, S. Y. Lee, J. A. Jeong, M. H. Lee, and T. S. Baek, *Corros. Sci. Tech.*, **13**, 20 (2014).
16. D. H. Jeon, *Corrosion and Corrosion control*, p. 220, Il Jung Publication Co. Ltd., Pusan (1985).